Ultrafast Diffraction

DOI: 10.1002/anie.200804152

Ultrafast Electron Diffraction Reveals Dark Structures of the Biological Chromophore Indole**

*Sang Tae Park, Andreas Gahlmann, Yonggang He, Jonathan S. Feenstra, and Ahmed H. Zewail**

Ultraviolet (UV) photodamage of biological chromophores, such as nucleic acid bases and amino acids, is critically controlled by the relaxation pathways following the initial excitation.[1–12] Photostability as a concept involves "dark structures",[13] which undergo photophysical and/or photochemical pathways.[14] Of major relevance is the time scale of structural change, since long-lived species would not be desirable for the photostability. Hence, it is important to identify the photophysical (intersystem crossing (ISC) and internal conversion (IC)) and photochemical (e.g. hydrogen atom abstraction) processes involved, and the associated structural transformations. These structures are not amenable to detection by conventional optical probing methods. Herein, we report our first ultrafast electron diffraction (UED) study of the structural dynamics of indole, the UV chromophore of the amino acid tryptophan.

Being an important fluorescence probe in protein studies,[15] tryptophan has been the subject of many spectroscopic investigations. The chromophore indole has complicated excited-state interactions and the photophysics and photochemistry vary depending on the excess energy. In the isolated molecule, the fluorescence quantum yield and lifetime on the nanosecond time scale were studied, when the molecule was excited around the origin of the first excited state (283.78 nm).[16] When excited at shorter wavelengths (below 271 nm), broad and structureless features in the electronic spectrum suggest the onset of an ultrafast nonradiative process of unknown nature.[17–22] Using time-resolved photoelectron spectroscopy, this ultrafast process was not observed, possibly due to cross-section consideration.[23] However, at higher energies the H-atom loss channel was observed at 193/248 nm[24] and below 260 nm.[25] The calculations of conical intersections between the singlet excited states and the $^1\pi\sigma^*$ repulsive state[26–28] have in fact predicted such behavior.

With UED, as detailed in the experimental section, we are able to determine both ground- and excited-state structures and obtain the temporal behavior for excitation of indole at 267 nm. For the ground-state structure (see Scheme SI1 in the Supporting Information), the experimental and the theoretical molecular scattering function, $sM(s)$, together with the radial distributions, $f(r)$, are shown in Figure 1. The refined structural parameters are listed in Table SI1 in the Supporting Information, together with values obtained from density functional theory (DFT) calculations. The satisfactory agreement between experiment and theory gives the refined structural parameters, which were found to have discrepancies at most within 0.007 Å and 0.1° for bond lengths and angles, respectively.

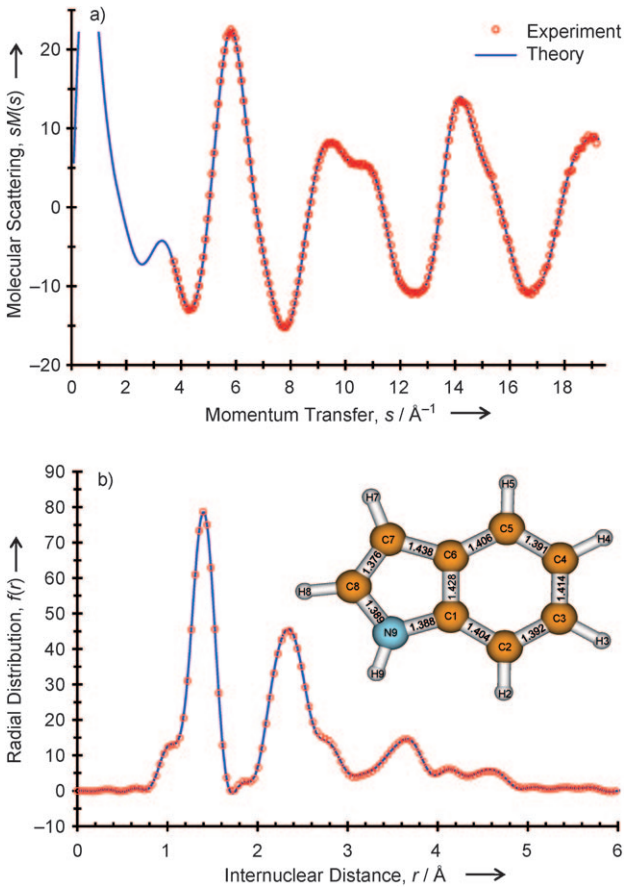

Figure 1. UED determined molecular structure of indole in the ground state. Shown are a) the molecular scattering function, $sM(s)$, and b) the radial distribution, $f(r)$, for the experimental (points) and theoretical curves (line). The maximum discrepancies are 0.007 Å and 0.1° for bond lengths and angles, respectively.

[*] Dr. S. T. Park, A. Gahlmann, Dr. Y. He, Dr. J. S. Feenstra, Prof. A. H. Zewail
Physical Biology Center for Ultrafast Science and Technology, Arthur Amos Noyes Laboratory of Chemical Physics, California Institute of Technology, 1200 E. California Blvd., Pasadena, CA 91125 (USA)
Fax: (+1) 626-796-8315
E-mail: zewail@caltech.edu

[**] This work was supported by the National Science Foundation and the Air Force Office of Scientific Research in the Gordon and Betty Moore Center of Physical Biology at Caltech. We would like to thank Prof. Kenneth W. Hedberg for help in designing the air-heated inlet system. We would also like to thank Prof. Andrzej L. Sobolewski for providing the starting geometries of the relevant species for our data analysis.

Supporting information for this article is available on the WWW under http://dx.doi.org/10.1002/anie.200804152.

The ground state of indole clearly exhibits some aromatic character in both the six- and five-membered rings. The C–C and the C–N bond lengths were determined with the values given in Figure 1; they all are in the range of 1.376 to 1.438 Å. However, the six-membered ring shows a slight "quinoid" character with elongated bond lengths of C3–C4 and C6–C1. The structure of the five-membered ring is very similar to that of pyrrole, except for the shared bond C6–C1, which is somewhat stretched. The aromaticity in the five-membered ring is maintained via conjugated π orbitals with the six-membered ring. This delocalization of π electrons results in the slight quinoid character of the six-membered ring.

For studies of structural dynamics following UV excitation, we recorded time-resolved diffraction patterns at different times, from −100 ps to +1 ns. The experimental frame-referenced $\Delta sM(s)$ curves are compared to the theoretical ones for the possible structures involved (see Figure SI1). Theoretical structures of the L_b, L_a, T_2, hot S_0 state and photoproducts (H-atom loss), are excluded on our time scale, because of the relatively poorer fits. The best fit was obtained using the structure of the T_1 state as the product (Figure SI1d). We also performed multicomponent fits by floating the fraction of several channels at once. In this way, the T_1 structure was exclusively favored at all time points.

With the major reaction channel identified, the structure was then refined (listed in Table SI2). Figure 2a displays the experimental product-only $f(r)$ curve with the theory at the +100 ps time delay (frame referenced at −100 ps). The ππ* character of the T_1 state is readily seen from the broken aromaticity, which results in distinctly alternating single and double bonds. From the temporal frame-referenced diffraction data, the population of this product structure as a function of time was determined, and the result for the temporal change of the fraction is shown in Figure 2b. A nonlinear fit of an exponential function, for a single-step process, gives a rise time of 6.3 ± 1.1 ps.

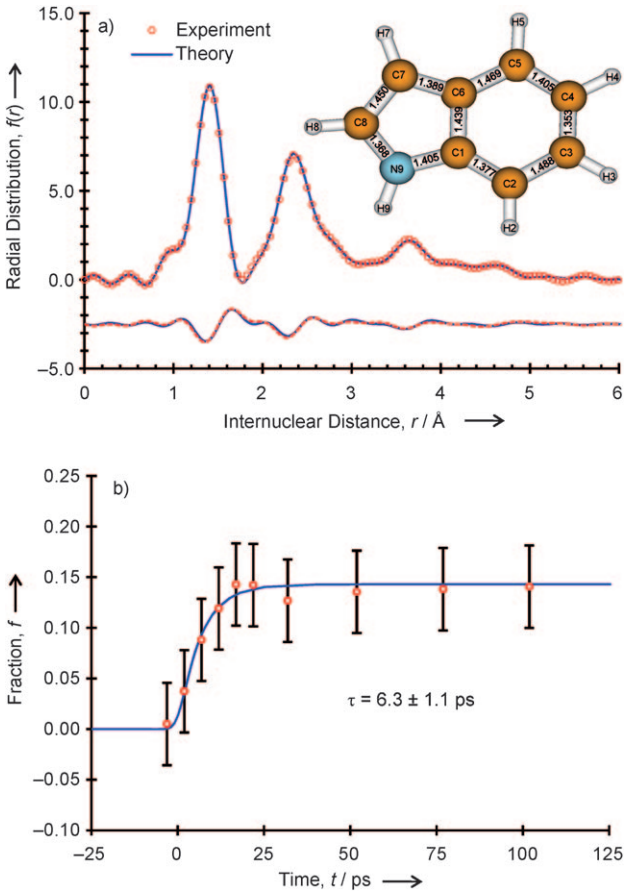

Figure 2. UED determined excited-state structure, following UV excitation. a) Product-only radial distribution curve, $f(r; t{=}{+}100\text{ ps})$, for indole with T_1 as a product. Also shown in the lower trace is the frame-referenced radial distribution curve, $\Delta f(r; t{=}{+}100\text{ ps}, t_{ref}{=}{-}100\text{ ps})$. b) Temporal evolution of the fraction of the product. The rise gives $\tau = 6.3 \pm 1.1$ ps.

The structural dynamics following 267 nm excitation thus indicate that the triplet-state channel is significant in the depopulation of the initial structure. The previous spectroscopic studies on indole and substituted indoles, which reported a complete loss of vibronic structure above the S_1 origin,[17–22] a feature reflective of a short-lived species at this energy,[20,29] can now be understood in relation to our findings. Of particular interest to the present study are the reported drop-off of the fluorescence yield at ca. 900 cm^{-1} above the origin of 3-methylindole, which has been attributed to an accelerated rate of ISC,[18] and the broad band of the NH stretching mode in the S_1 state,[29] which suggests a longer than 3 ps lifetime at an excess energy (3478 cm^{-1} above S_1) comparable to ours (ca. 5000 cm^{-1} including thermal energy; energy redistribution lowers this value for the coordinate of interest).

The rise time of 6.3 ps for the triplet state, determined by UED, may appear rather short given the fact that ISC, in this case of 267 nm excitation, is between ππ* singlet and triplet states. However, this symmetry and parity rule[30] is normally applicable for a planar geometry and, when nonplanar distortions are involved, vibronic couplings must be included.[31] It has been shown in the case of cytosine that significant spin–orbit coupling, and consequently efficient ISC, can occur, provided the $^1\pi\pi^*$ and $^3\pi\pi^*$ states cross at a nonplanar geometry.[32]

In order to test such a conjecture for indole, we carried out calculations at the CASSCF(12,11)/6-311G(d,p) level and found that the T_2 ($^3\pi\pi^*$) state of indole possesses a nonplanar equilibrium geometry. Furthermore, T_2 ($^3\pi\pi^*$) crosses S_1 at near 828 cm^{-1} above the S_1 origin with a quasi-nonplanar geometry at the point of crossing. The proximity of the crossing point to the S_1 energy minimum enhances the Franck–Condon overlap,[33,34] resulting in ultrafast ISC. It should be noted that the L_a and L_b states are heavily mixed, but at our wavelength the contribution of the L_a (S_2) state seems to be larger than that of L_b (S_1).[35] We observe the final structure in the T_1 state in 6.3 ps, which suggests that T_2 and T_1 mixing/conversion is very efficient. Future experiments with polarized photoselection[36] would address such a state mixing effect on UED.[37,38]

In Figure 3, we summarize the experimental and theoretical findings on the indicated potential energy curves for indole. In this picture, the S_1 and T_2 states cross right above the S_1 origin, whereas singlet and triplet ππ* states cross with

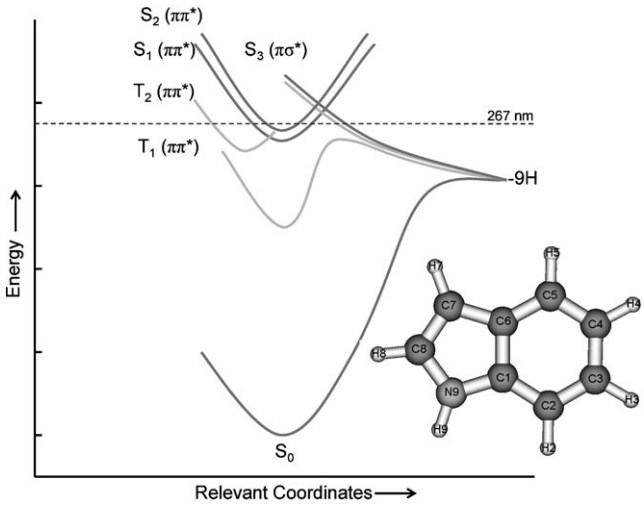

Figure 3. Potential energy curves of the excited and ground states of indole along the hydrogen-atom loss and bound effective coordinates. For discussion of the excited states involved, see text.

the πσ*,[26–28] which leads to H-atom loss at higher energies. On our time scale, for the 267 nm excitation, it can thus be concluded that the involvement of the repulsive ^{1}πσ* state is minor. Above the $S_1/^1$πσ* crossing, which has been observed to be at ca. 260 nm,[25] a competition between ISC to the triplet manifold and IC to the ^{1}πσ* state would take place, perhaps with the latter dominating at high energies. The long-lived T_1 state can also lose an H-atom over a shallow reaction barrier but on a longer timescale. The slow component of H-atom loss, observed at 248 nm in the mass spectrometry study,[24] may accordingly originate from the T_1 state, because the ground-state reaction would be too slow to be observed.

In conclusion, the structural dynamics reported herein for the tryptophan chromophore (indole) using ultrafast electron diffraction reveals the involvement of triplet state(s) in the nonradiative pathway of excited states. The product, excited triplet, has a broken aromatic structure, whereas the ground-state structure was determined to have aromaticity both for the six- and five-membered rings, with a slight "quinoid" character; the C–C and the C–N bond distances were thus determined and they are in the range from 1.376 to 1.438 Å. The rate of product formation is 1.6×10^{11} s^{-1}, which accounts for the broad spectra observed in the excited state. This perspective from the UED study on the photophysics and photochemistry of indole emphasizes the direct role of intermediate dark structures in the overall relaxation pathways. Partial population of these states has to be taken very seriously in addressing photostability of biological chromophores. Moreover, given the involvement of reactive triplets, the solvent effect, especially water, will have to be integrated into any picture of the dynamics and stability.

Experimental Section

A detailed description of the UED-3 apparatus and data analysis has been given in previous publications.[39] Briefly, ultrashort laser pulses (120 fs) at 800 nm were frequency-tripled to generate the UV light (450 μJ/pulse), which was then split into two beam paths. The pump beam (ca. 93% of the total energy) was time delayed using a translation stage and was directed into the scattering chamber to initiate the reaction. The weaker beam (ca. 7% of the total energy) was attenuated, focused, and directed onto a back-illuminated silver-coated cathode to generate the ultrashort electron pulses (2.5×10^4 electrons/pulse at 30 keV) via the photoelectric effect. An effusive beam of indole was introduced into the chamber via our newly implemented, air-heated inlet system at 543 K. Indole (>99%) was purchased from Aldrich and used without further purification.

The starting geometries for structural analysis were obtained from quantum chemical calculations using approximated singles and doubles coupled-cluster (CC2) method with the aug-cc-pVTZ basis set, and density functional theory calculations at the B3LYP/6–311G(d,p) level using Gaussian 98 suite.[40] Structural analysis was conducted using home-built software, following the methodology described previously.[39] We have also implemented the redundant-internal-coordinate[41,42] system and the correlation-elimination method[43] by near-singularity removal in our UED analysis.

Received: August 22, 2008
Published online: November 5, 2008

Keywords: amino acids · biological photodamage · biological structures · electron diffraction · intersystem crossing

[1] A. L. Sobolewski, W. Domcke, *J. Phys. Chem. A* **2007**, *111*, 11725–11735.
[2] T. J. Martinez, *Acc. Chem. Res.* **2006**, *39*, 119–126.
[3] H. R. Hudock, B. G. Levine, A. L. Thompson, H. Satzger, D. Townsend, N. Gador, S. Ullrich, A. Stolow, T. J. Martinez, *J. Phys. Chem. A* **2007**, *111*, 8500–8508.
[4] B. Kohler, *Photochem. Photobiol.* **2007**, *83*, 592–594.
[5] C. E. Crespo-Hernández, B. Cohen, P. M. Hare, B. Kohler, *Chem. Rev.* **2004**, *104*, 1977–2019.
[6] P. M. Hare, C. E. Crespo-Hernández, B. Kohler, *J. Phys. Chem. B* **2006**, *110*, 18641–18650.
[7] P. R. Callis, *Annu. Rev. Phys. Chem.* **1983**, *34*, 329–357.
[8] D. Creed, *Photochem. Photobiol.* **1984**, *39*, 537–562.
[9] D. Creed, *Photochem. Photobiol.* **1984**, *39*, 563–575.
[10] D. Creed, *Photochem. Photobiol.* **1984**, *39*, 577–583.
[11] J. Peon, A. H. Zewail, *Chem. Phys. Lett.* **2001**, *348*, 255–262.
[12] S. K. Pal, J. Peon, A. H. Zewail, *Chem. Phys. Lett.* **2002**, *363*, 57–63.
[13] R. Srinivasan, J. S. Feenstra, S. T. Park, S. J. Xu, A. H. Zewail, *Science* **2005**, *307*, 558–563.
[14] J. Michl, V. Bonačić-Koutecký, *Electronic Aspects of Organic Photochemistry*, Wiley, New York, **1990**.
[15] J. R. Lakowicz, *Principles of Fluorescence Spectroscopy*, 2nd ed., Plenum, New York, **1999**.
[16] R. J. Lipert, G. Bermudez, S. D. Colson, *J. Phys. Chem.* **1988**, *92*, 3801–3805.
[17] R. Bersohn, U. Even, J. Jortner, *J. Chem. Phys.* **1984**, *80*, 1050–1058.
[18] T. R. Hays, W. E. Henke, H. L. Selzle, E. W. Schlag, *Chem. Phys. Lett.* **1983**, *97*, 347–351.
[19] J. Hager, S. C. Wallace, *J. Phys. Chem.* **1983**, *87*, 2121–2127.
[20] J. W. Hager, D. R. Demmer, S. C. Wallace, *J. Phys. Chem.* **1987**, *91*, 1375–1382.
[21] D. M. Sammeth, S. Yan, L. H. Spangler, P. R. Callis, *J. Phys. Chem.* **1990**, *94*, 7340–7342.
[22] K. W. Short, P. R. Callis, *Chem. Phys.* **2002**, *283*, 269–278.
[23] H. Lippert, H.-H. Ritze, I. V. Hertel, W. Radloff, *Chem. Phys. Lett.* **2004**, *398*, 526–531.
[24] M.-F. Lin, C.-M. Tseng, Y. T. Lee, C.-K. Ni, *J. Chem. Phys.* **2005**, *123*, 124303.

[25] M. G. D. Nix, A. L. Devine, B. Cronin, M. N. R. Ashfold, *Phys. Chem. Chem. Phys.* **2006**, *8*, 2610 – 2618.
[26] A. L. Sobolewski, W. Domcke, *Chem. Phys. Lett.* **1999**, *315*, 293 – 298.
[27] A. L. Sobolewski, W. Domcke, C. Dedonder-Lardeux, C. Jouvet, *Phys. Chem. Chem. Phys.* **2002**, *4*, 1093 – 1100.
[28] C. Dedonder-Lardeux, C. Jouvet, S. Perun, A. L. Sobolewski, *Phys. Chem. Chem. Phys.* **2003**, *5*, 5118 – 5126.
[29] B. C. Dian, A. Longarte, T. S. Zwier, *J. Chem. Phys.* **2003**, *118*, 2696 – 2706.
[30] M. A. El-Sayed, *J. Chem. Phys.* **1963**, *38*, 2834 – 2838.
[31] E. C. Lim, J. M. H. Yu, *J. Chem. Phys.* **1967**, *47*, 3270 – 3275.
[32] M. Merchán, L. Serrano-Andrés, M. A. Robb, L. Blancafort, *J. Am. Chem. Soc.* **2005**, *127*, 1820 – 1825.
[33] N. Matsunaga, S. Koseki, M. S. Gordon, *J. Chem. Phys.* **1996**, *104*, 7988 – 7996.
[34] C. M. Marian in *Rev. Comput. Chem.*, *Vol. 17* (Eds.: K. Lipkovitz, D. Boyd), Wiley-VCH, Weinheim, **2001**, pp. 99 – 204.
[35] E. Jalviste, N. Ohta, *J. Chem. Phys.* **2004**, *121*, 4730 – 4739.
[36] B. Albinsson, B. Nordén, *J. Phys. Chem.* **1992**, *96*, 6204 – 6212.
[37] J. S. Baskin, A. H. Zewail, *ChemPhysChem* **2005**, *6*, 2261 – 2276.
[38] J. S. Baskin, A. H. Zewail, *ChemPhysChem* **2006**, *7*, 1562 – 1574.
[39] S. T. Park, J. S. Feenstra, A. H. Zewail, *J. Chem. Phys.* **2006**, *124*, 174707.
[40] M. J. Frisch, et al., Gaussian Inc., Pittsburgh, PA, **1998**.
[41] S. Califano, *Vibrational States*, Wiley, New York, **1976**.
[42] E. B. Wilson, Jr., J. C. Decius, P. C. Cross, *Molecular Vibrations: The Theory of Infrared and Raman Vibrational Spectra*, McGraw-Hill, New York, **1955**.
[43] W. H. Press, S. A. Teukolsky, W. T. Vetterling, B. P. Flannery, *Numerical Recipe in Fortran: The Art of Scientific Computing*, 2nd ed., Cambridge University Press, Cambridge, **1992**.

